Labeling Where Adapting Fails: Cross-Domain Semantic Segmentation with Point Supervision via Active Selection

Fei Pan
KAIST
feipan@kaist.ac.kr

Francois Rameau
KAIST
frameau@kaist.ac.kr

Junsik Kim
Harvard University
mibastro@gmail.com

In So Kweon
KAIST
iskweon77@kaist.ac.kr

Abstract

Training models dedicated to semantic segmentation requires a large amount of pixel-wise annotated data. Due to their costly nature, these annotations might not be available for the task at hand. To alleviate this problem, unsupervised domain adaptation approaches aim at aligning the feature distributions between the labeled source and the unlabeled target data. While these strategies lead to noticeable improvements, their effectiveness remains limited. To guide the domain adaptation task more efficiently, previous works attempted to include human interactions in this process under the form of sparse single-pixel annotations in the target data. In this work, we propose a new domain adaptation framework for semantic segmentation with annotated points via active selection. First, we conduct an unsupervised domain adaptation of the model; from this adaptation, we use an entropy-based uncertainty measurement for target points selection. Finally, to minimize the domain gap, we propose a domain adaptation framework utilizing these target points annotated by human annotators. Experimental results on benchmark datasets show the effectiveness of our methods against existing unsupervised domain adaptation approaches. The propose pipeline is generic and can be included as an extra module to existing domain adaptation strategies.

1. Introduction

Semantic segmentation consists in assigning every image's pixel with its corresponding semantic class. With the recent improvements brought by convolution neural networks [26, 6, 51], semantic segmentation finds applications in a wide spectrum of tasks, such as, autonomous driving [27, 49], robotics [31] and disease diagnostic [53, 50]. Training semantic segmentation model is a data hungry process where a large number of pixel-wise annotated images is required. Typically, these annotations are manually assigned by human operators, which makes this task
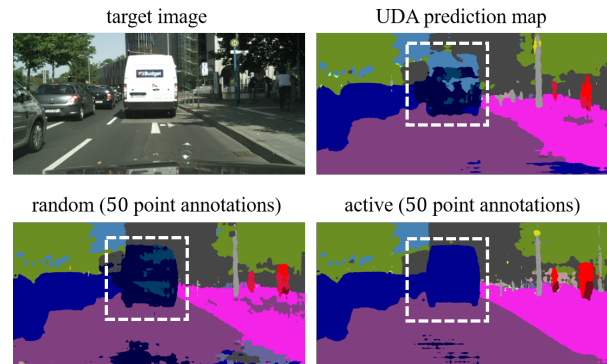

Figure 1: Existing UDA approaches' performance remains limited when the domain gap is big. We propose a domain adaptation framework for semantic segmentation with annotated target points via active selection. Under same labeling budget (50 point annotations), our approach utilizing point annotations via active selection outperforms the random selection method.

cumbersome, time consuming and, as a result, particularly expensive [8]. While various computer applications have been successfully resolved in a self-supervised manner (such as, visual odometry [52] or depth estimation [17]), semantic segmentation still requires to be trained in a supervised fashion. Despite the availability of large scale annotated datasets for semantic segmentation [8, 48, 16], a network trained with this data is not guaranteed to generalize to a different set of images. This phenomenon is caused by the the distinct distributions between the two datasets, this discrepancy is known as *domain gap* [15]. To alleviate this problem, unsupervised domain adaptation (UDA) strategies have been proposed to align the feature distributions between the labeled source data and the unlabeled target data [32, 40, 34, 19]. Specifically, adversarial learning-based UDA approaches has shown efficiency in aligning the domain gap at image [19], features [38] or output level [43, 44]. While UDA approaches lead to noticeable improvements, their effectiveness remains limited.

This remaining performance gap significantly diminish the relevance and practicability of these techniques for real-world applications where a high level of accuracy is required. To reduce the domain gap further, domain adaptation coupled with weak human annotation have been developed [35, 47]. Instead of performing a full pixel-wise annotations of the target images, weak labeling consists in simpler and faster tasks, for instance, bounding box selection [10, 33], image-level [1, 5, 23] or points-level [2] annotations. The cost of these weak annotations is significantly lower than their dense counterpart, making it realistically deplorable for industrial and commercial purpose. However, we argue that existing annotation process is yet to be optimized to achieve better performance under same labeling budget.

In this work, we propose a new domain adaptation framework for semantic segmentation with annotated points via active selection. Our framework consists of three parts, which are presented in Figure 2, namely, 1) an unsupervised domain adaptation to train a segmentation network and generates the entropy maps and predicted segmentation maps for all target training images, 2) an entropy-based label acquisition system to request annotations for points with high uncertainty level from oracle, while transferring UDA predicted labels to pseudo labels for points with low uncertainty level, 3) a new domain adaptation framework with target weak annotations to further align the domain shift. Our proposed approach achieves good performance against state-of-the-art UDA approaches on benchmark datasets.

The Contributions of Our Work. First, we introduce an entropy-based label acquisition method which is optimized to achieve better segmentation performance under equal labeling budget. Second, we propose a new domain adaptation model with target point-based weak annotations for semantic segmentation task.

2. Related Works

In this section, we describe related methods for unsupervised domain adaptation and weakly supervised semantic segmentation. Moreover, we discuss about recent uncertainty estimation via entropy, which is a central component of the proposed technique.

Unsupervised Domain Adaptation. Unsupervised domain Adaptation (UDA) approaches aim at aligning the distribution shift between the labeled source data and the unlabeled target data. Recently, adversarial-based UDA approaches [34, 32, 45, 44, 19, 43] have demonstrated to be effective in learning domain invariant features for semantic segmentation task. Adversarial-based UDA approaches for semantic segmentation contain two networks, one network is used as a generator to predict the segmentation maps of

input images, which is given from either the source domain or target domain. Based on this, the second network, as a discriminator, predicts the domain labels for the features given from the generator. Then the generator tries to fool the discriminator, so as to align the distribution shift of features from the two domains. Besides alignment on feature level, other approaches propose to align domain shift at the image level [19], output level [43] or entropy level [45]. More recently, [44] proposes to align the domain shift by utilizing the patch-wise output distribution from the two domains. While existing UDA approaches lead to noticeable improvements, their effectiveness remains limited when the domain shift is large. In this paper, we combine a UDA approach with small labeling budget, *i.e.* point annotation, to align domain gap effectively.

Weakly Supervised Semantic Segmentation. Weakly supervised semantic segmentation approaches utilize various types of weak semantic labels including image-level labels [1, 5, 23], bounding box [10, 33], scribble labels [25], and point labels [2]. These approaches propose to train a segmentation model with these weak labels and test it in the same domain. Based on their frameworks, [47] proposes to combine target bounding box annotation with domain adaptation to improve semantic segmentation performance from the source domain to the target domain. [35] takes advantage of target weak point annotations with domain adaptation for better domain alignment. While existing approaches utilize target weak labels to reduce labeling cost in domain adaptation for semantic segmentation task, they fail to consider an optimized weak labeling policy. In this work, we propose a domain adaptation framework with point supervision via active selection to make the annotation process even more efficient.

Uncertainty via Entropy. Entropy as a measurement of uncertainty has been used in domain adaptation. [45] takes advantage of entropy of pixel-wise segmentation output to align the domain shift. Based on this, [32] proposes entropy-based ranking system to split the target domain into two distinct parts: the easy and hard split. On this basis, an inter-domain and intra-domain adaptation are conducted to minimize the domain shift. Recently, [42] adopts the entropy of output as a confidence measurement for transferring samples across domains. Entropy functions as a uncertainty measurement has also been used widely in active learning for image recognition [28, 39, 20]. There are a few works proposed recently applying active learning for semantic segmentation. [21] applies entropy-based uncertainty measurement on super-pixels to find important regions to be labelled, then apply a conditional random field to propagate labels. Similarly, [41] proposes to use a view-point entropy combined with super-pixels to select

informative samples for multi-view semantic segmentation. [30] use vote entropy [9] from dropout layers of segmentation model by constructing a Monte-Carlo dropout ensemble [14]. While a number of works dedicated their effort to the efficient annotation for semantic segmentation, their scenarios are limited to a single domain.

The effort to reduce the labeling budget has been researched in different directions separately: UDA, use of weak labels and active sampling. Although they aim for the same goal, *i.e.*, reducing labeling cost, an attempt to harmonize these approaches has not been explored yet. We propose an active sampling of weak labels under a domain adaptation scenario suggesting a new important research direction.

3. Methodology

In this section, a cross-domain semantic segmentation approach using target point annotations via an active selection is introduced. The proposed approach consists of three parts. First, a cross-domain segmentation model [6] G_1 is trained using the labeled source data and the unlabeled target data. The model G_1 takes each target data to generate prediction maps and entropy maps. Secondly, an entropy-based uncertainty measurement is used to automatically select ambiguous patches in the target images and request for point annotation from oracles. Lastly, a simple yet effective domain adaptation method using target weak and pseudo-label annotations to train a second semantic segmentation model [6] G_2 is proposed.

Let $\mathcal{S}$ denote a source domain containing a set of RGB images and their corresponding pixel-wise annotations $\{X_s^i, Y_s^i\}_{s=1}^{N_s}$, where $X_s^i \in \mathbb{R}^{H \times W \times 3}$, $Y_s^i \in \mathbb{R}^{H \times W \times C}$; where N_s and C stands for to the number of image-label pairs and the number of classes (for both source domain and target domain), respectively. Similarly, let $\mathcal{T}$ denote a target domain containing a set of unlabelled images $\{X_t^i\}_{t=1}^{N_t}$, where $X_t^i \in \mathbb{R}^{H \times W \times 3}$ and N_t is the number of target data.

3.1. Unsupervised Domain Adaptation

It is assumed that the target domain exclusively contains unlabeled RGB images before any request for annotations from oracle. In order to estimate the adaptation uncertainty on the target data, an unsupervised domain adaptation (UDA) is conducted using a semantic segmentation model G_1. Given a sample X_s from the source domain alongside with its ground-truth annotation Y_s, the network G_1 takes X_s as an input and generates a "soft-segmentation map" $P_s = G_1(X_s)$. In this map, each C dimensional vector $\left[P_s^{(h,w,c)}\right]_C$ at a pixel position (h,w) is a discrete probability distribution over C classes. The segmentation model

G_1 is optimized through a cross-entropy loss:

$$\mathcal{L}_{seg}^1(X_s, Y_s) = - \sum_{h,w,c} Y_s^{(h,w,c)} \log P_s^{(h,w,c)}. \quad (1)$$

To bridge the domain gap between the source and the target domain, ADVENT [45] aligns the entropy maps from the source domain and the target domain by using an adversarial training technique. The assumption of [45] is that the trained models tend to produce high-confident (low-entropy) predictions on source-like data, and low-confident (high-entropy) predictions on target-like data. Given an input X_t from the target domain, the segmentation model G_1 produces the segmentation map $P_t = G_1(X_t)$. The entropy map $E \in \mathbb{R}^{H \times W \times C}$ is formulated as:

$$E_t^{(h,w,c)} = -P_t^{(h,w,c)} \log P_t^{(h,w,c)}. \quad (2)$$

In order to align features from the source domain and the target domain, a domain discriminator D_1 is trained to produce a domain label given the entropy map as an input. In other words, D_1 produces 1 when the entropy map is from source domain, and 0 when it is from the target domain. On this basis, G_1 is trained to fool D_1. The optimization of G_1 and D_1 is achieved by the adversarial loss function:

$$\mathcal{L}_{adv}^1(X_s, X_t) = \sum_{h,w,c} \log[1 - D_1(E_t^{(h,w,c)})] \\ + \log D_1(E_s^{(h,w,c)}), \quad (3)$$

where E_s is the entropy map of X_s. The complete loss function of unsupervised domain adaptive segmentation is formulated as:

$$\min_{G_1} \max_{D_1} \mathcal{L}_{seg}^1(X_s, Y_s) + \mathcal{L}_{adv}^1(X_s, X_t). \quad (4)$$

3.2. Label Acquisition

Due to a large domain gap, the segmentation model G_1 trained on labeled source data and unlabeled target data might still lead to poor performance on the target domain. In order to reduce the domain gap further, we propose to use additional information from human annotators on the target data. For monetary reasons [2], instead of relying on dense annotations, oracles are requested to provide point-level weak annotations on the target data. Concretely, an target image containing a single landmark point is provided to the annotator who has to select the class corresponding to this pixel. While the location of these points is sometimes assigned randomly [35]. In this work, we designed an entropy-based selection method to automatically select the most informative points to be annotated. Once the segmentation model G_1 is optimized via (4), given a target image X_t as an input, G_1 generates its segmentation map P_t and entropy map E_t. This entropy map is used to locate the most
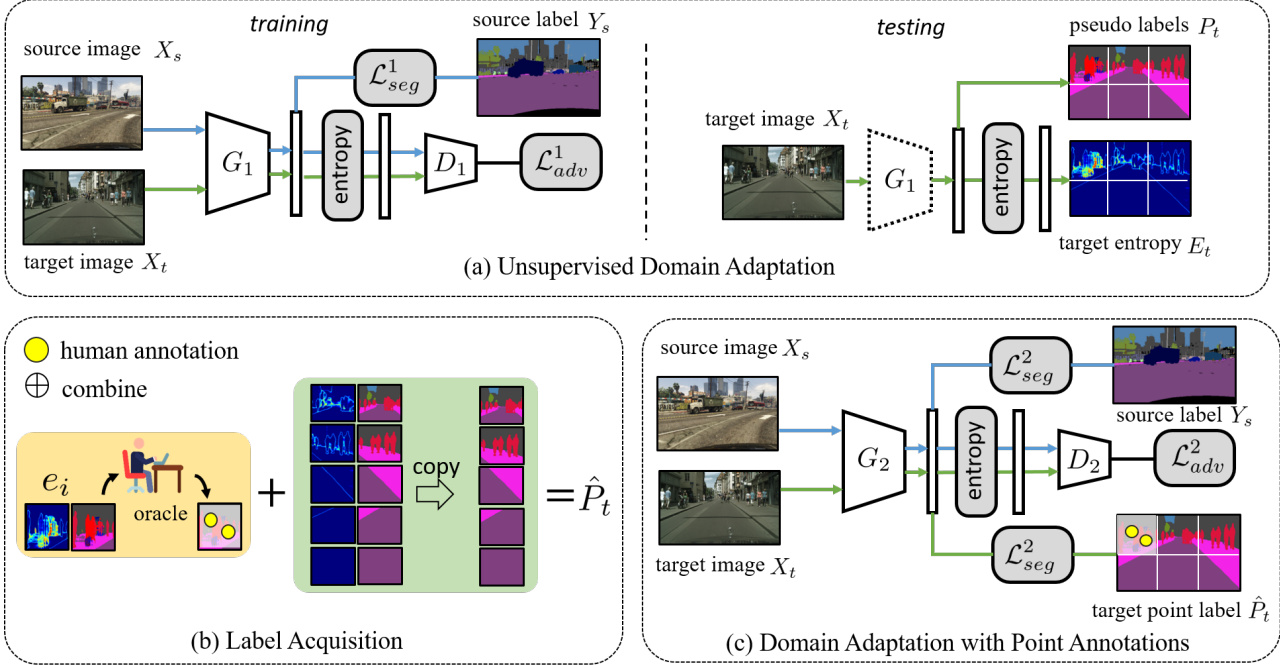
Figure 2: The proposed cross-domain semantic segmentation approach using target point annotations via active selection consists of three parts, namely, (a) an unsupervised domain adaptation (b) a label acquisition system, and (c) a domain adaptation using target point annotations. In (a), given the labeled source data and unlabeled target data, a segmentation model [6] G_1 is trained to generate prediction maps as pseudo labels and entropy maps; D_1 is trained to predict the domain label for the entropy maps while G_1 is trained to fool D_1. $\{G_1, D_1\}$ are optimized by minimizing the segmentation loss $\mathcal{L}^1_{seg}$ and the adversarial loss $\mathcal{L}^1_{adv}$. In (b), an entropy-based label acquisition system is used to locate the most uncertain predictions in the target image, on which a human annotation is pertinent. The yellow dots represents locations of the selected points for human annotation, while in other patches the pseudo labels are copied and preserved. In (c), a domain adaption method with point annotations from target domain is proposed. Given the data from both domains, the semantic segmentation model G_2 is trained to generate predictions maps and entropy maps. D_2 is used to predict whether the samples is from the source domain or the target domain, while G_2 is used to fool D_2. $\{G_2, D_2\}$ is optimized using a cross-entropy based segmentation loss $\mathcal{L}^2_{seg}$ and adversarial loss $\mathcal{L}^2_{adv}$.

uncertain predictions in the image X_t on which a human annotation would be pertinent. Specifically, E_t is divided by a $M \times N$ regular grid into multiple patches $\{e^i_t\}^{M \times N}_{i=1}$, where $E_t = \{e^i_t\}^{M \times N}_{i=1}$. Note that $e^i_t \in \mathbb{R}^{H' \times W' \times C}$, where H' and W' are the height and width of patches. In order to localize the uncertainty prediction area on target data, we take consideration of the mean entropy e^i of the patch, which is given by:

$$\epsilon^i = \sum_{h',w',c} e^{i(h',w',c)}_t. \qquad (5)$$

As an uncertainty measurement, ϵ^i with a high value suggests that the model G_1 produce high uncertainty predictions in the cell e^i_t. Thus, an oracle is requested to label one (or multiple) points in the most uncertain patches of the image. Given a selected patch e^i_t, a random point position $\{a, b\}$ is chosen inside the patch; If ϵ^i is among the top

K highest mean entropy among all patches, then a request is sent for oracles to label the point positions $\{a, b\}$; otherwise, the pseudo label from the predicted map P_t (from UDA) will be transferred at $\{a, b\}$ as this prediction is assumed to be confident. While for all the other non-selected patches, we directly copy its pseudo labels, as shown in the green area of 2 (b). Let $\hat{P}_t$ denote a new label, the annotation process is formulated as follows:

$$\hat{P}_t(e^i_t) = \begin{cases} \text{oracle,} & \text{if } \epsilon^i_t \in \text{top } K \text{ highest} \\ P_t(e^i_t), & \text{otherwise} \end{cases} . \qquad (6)$$

3.3. Domain Adaptation with Weak Annotations

In this section, a domain adaptation method using target weak annotations $\hat{P}_t$ to train a semantic segmentation network G_2 is introduced. In order adapt the segmentation

Table 1: The semantic segmentation results of Cityscapes validation set with trained models adapted from GTA5 to Cityscapes. All the results are generated from the ResNet-101-based models. IntraDA [32] is used as our UDA baseline model for the experiments. Self-training denotes the performance generated from experiments by only using pseudo labels from first stage of IntraDA. Random selection denotes the performance generated from experiments by randomly selecting 10 patches with each 5 human point annotations are provided. Active selection denotes the performance generated from experiments by selecting top 10 highest entropy patches with each 5 human point annotations are provided. Full labeling denotes the performance generated from experiments by selecting top 10 highest patches with each full human point annotations are provided. mIoU denotes the mean IoU over 19 classes.

| | GTA5 → Cityscapes | | | | | | | | | | | | | | | | | | | |
Method	road	sidewalk	building	wall	fence	pole	light	sign	veg	terrain	sky	person	rider	car	truck	bus	train	mbike	bike	mIoU
No Adaptation [43]	75.8	16.8	77.2	12.5	21.0	25.5	30.1	20.1	81.3	24.6	70.3	53.8	26.4	49.9	17.2	25.9	6.5	25.3	36.0	36.6
ROAD [7]	76.3	36.1	69.6	28.6	22.4	28.6	29.3	14.8	82.3	35.3	72.9	54.4	17.8	78.9	27.7	30.3	4.0	24.9	12.6	39.4
AdaptSegNet [43]	86.5	36.0	79.9	23.4	23.3	23.9	35.2	14.8	83.4	33.3	75.6	58.5	27.6	73.7	32.5	35.4	3.9	30.1	28.1	42.4
CLA [29]	87.0	27.1	79.6	27.3	23.3	28.3	35.5	24.2	83.6	27.4	74.2	58.6	28.0	76.2	33.1	36.7	6.7	31.9	31.4	43.2
MinEnt [45]	84.2	25.2	77.0	17.0	23.3	24.2	33.3	26.4	80.7	32.1	78.7	57.5	30.0	77.0	37.9	44.3	1.8	31.4	36.9	43.1
AdvEnt [45]	89.9	36.5	81.6	29.2	25.2	28.5	32.3	22.4	83.9	34.0	77.1	57.4	27.9	83.7	29.4	39.1	1.5	28.4	23.3	43.8
SWD [24]	92.0	46.4	82.4	24.8	24.0	35.1	33.4	34.2	83.6	30.4	80.9	56.9	21.9	82.0	24.4	28.7	6.1	25.0	33.6	44.5
SSF-DA [12]	90.3	38.9	81.7	24.8	22.9	30.5	37.0	21.2	84.8	38.8	76.9	58.8	30.7	85.7	30.6	38.1	5.9	28.3	36.9	45.4
DISE [4]	91.5	47.5	82.5	31.3	25.6	33.0	33.7	25.8	82.7	28.8	82.7	62.4	30.8	85.2	27.7	34.5	6.4	25.2	24.4	45.4
IntraDA [32]	90.6	36.1	82.6	29.5	21.3	27.6	31.4	23.1	85.2	39.3	80.2	59.3	29.4	86.4	33.6	53.9	0.0	32.7	37.6	46.3
AdaptPatch [44]	92.3	51.9	82.1	29.2	25.1	24.5	33.8	33.0	82.4	32.8	82.2	58.6	27.2	84.3	33.4	46.3	2.2	29.5	32.3	46.5
Self-training (lower bound)	91.8	50.1	84.7	33.3	28.1	30.3	36.9	29.1	84.1	34.2	86.4	60.1	31.8	83.1	25.5	46.7	0.0	28.1	40.2	47.7
Ours - Random Selection	92.2	51.7	84.8	32.8	28.2	31.0	37.6	31.2	84.2	35.1	85.3	61.7	32.3	83.2	29.4	49.3	0.2	33.5	42.3	48.7
Ours - Active Selection	92.7	55.6	85.4	35.9	30.5	33.7	40.2	35.0	85.2	38.9	86.3	63.9	36.5	84.6	30.7	49.3	1.8	38.2	54.7	51.5
Ours - Full Labeling (upper bound)	94.9	68.4	86.2	42.3	36.1	37.7	39.8	52.4	86.9	47.6	88.6	64.6	40.4	88.6	59.8	65.5	40.0	40.3	61.1	**60.1**

model G_2 into the target domain, we use target weak annotations to optimize G_2 via a cross-entropy loss. Given a sample X_s from the source domain and X_t from the target domain, we forward them into G_2 and obtain the segmentation maps $P'_s = G_2(X_s)$ and $P'_t = G_2(X_t)$. With the aid of the source annotation Y_s and the target weak annotation $\mathcal{Y}_t$, the segmentation model G_2 is optimized by the segmentation loss:

$$\mathcal{L}^2_{seg}(X_s, Y_s, X_t, \hat{P}_t) = -\sum_{h,w,c} Y_s^{(h,w,c)} \log G_2(X_s^{(h,w,c)})$$
$$+ \hat{P}_t^{(h,w,c)} \log G_2(X_t^{(h,w,c)}). \quad (7)$$

To bridge the gap between the source domain and the target domain, we adopt an entropy-based alignment strategy for both domains. Given the predicted maps P'_s and P'_t, we calculate the corresponding entropy maps E'_s and E'_t by using (2). To close the domain gap, a discriminator D_2 is trained to predict the domain labels of E'_s and E'_t. And G_2 is trained to fool D_2. The adversarial training loss to optimize G_2 and D_2 is given by:

$$\mathcal{L}^2_{adv}(X_s, X_t) = \sum_{h,w,c} \log[1 - D_1(E'^{(h,w,c)}_t)]$$
$$+ \log D_1(E'^{(h,w,c)}_s). \quad (8)$$

In the end, our complete loss function is formed by:

$$\mathcal{L} = \mathcal{L}^2_{seg}(X_s, Y_s, X_t, \hat{P}_t) + \mathcal{L}^2_{adv}(X_s, X_t). \quad (9)$$

Our goal is to learn a target segmentation model $G_2{}^*$ through:

$$G_2^* = \arg\min_{G_2} \min_{G_2} \max_{D_2} \mathcal{L}. \quad (10)$$

4. Experiments

4.1. Datasets

To evaluate our proposed approach with state-of-the-art UDA approaches [43, 45, 29, 24, 32], we adopt the same setting of adaptation from the synthetic to the real domain. To conduct this series of tests, synthetic datasets including GTA5 [36] and SYNTHIA [37] are used as source domains, along with the real-world dataset Cityscapes [8] as the target domain. In the training period, the models are given labeled source data and unlabeled target data as inputs. After training, the models are evaluated on Cityscapes validation set.

- GTA5: we adopt the synthetic dataset GTA5 [36] which contains 24,966 synthetic images and corresponding ground-truth annotations of $1,914 \times 1,052$. All of these synthetic images are generated from a video game engine which mimics the urban scenery of Los Angeles city. And the ground-truth annotations are produced automatically by programs from this game engine. The dataset covers a total of 33 classes. However, in consideration of the compatibility with the Cityscapes dataset, we use 19 out of 33 classes: road, sidewalk, building, wall, fence, pole,

Table 2: The semantic segmentation results of Cityscapes validation set with trained models adapted from SYNTHIA to Cityscapes. All the results are generated from the ResNet-101-based models. IntraDA [32] is used as our UDA baseline model for the experiments. Self-training denotes the performance generated from experiments by only using pseudo labels from first stage of IntraDA. Random selection denotes the performance generated from experiments by randomly selecting 10 patches with each 5 human point annotations are provided. Active selection denotes the performance generated from experiments by selecting top 10 highest entropy patches with each 5 human point annotations are provided. Full labeling denotes the performance generated from experiments by selecting top 10 highest patches with each full human point annotations are provided. mIoU denotes the mean IoU over 19 classes. mIoU* denotes the mean IoU of 13 classes, excluding the classes with *.

| | SYNTHIA → Cityscapes | | | | | | | | | | | | | | | | | |
Method	road	sidewalk	building	wall*	fence*	pole*	light	sign	veg	sky	person	rider	car	bus	mbike	bike	mIoU	mIoU*
No adaptation [43]	55.6	23.8	74.6	9.2	0.2	24.4	6.1	12.1	74.8	79.0	55.3	19.1	39.6	23.3	13.7	25.0	33.5	38.6
AdaptSegNet [43]	81.7	39.1	78.4	11.1	0.3	25.8	6.8	9.0	79.1	80.8	54.8	21.0	66.8	34.7	13.8	29.9	39.6	45.8
MinEnt [45]	73.5	29.2	77.1	7.7	0.2	27.0	7.1	11.4	76.7	82.1	57.2	21.3	69.4	29.2	12.9	27.9	38.1	44.2
AdvEnt [45]	87.0	44.1	79.7	9.6	0.6	24.3	4.8	7.2	80.1	83.6	56.4	23.7	72.7	32.6	12.8	33.7	40.8	47.6
CLAN [29]	81.3	37.0	80.1	-	-	-	16.1	13.7	78.2	81.5	53.4	21.2	73.0	32.9	22.6	30.7	-	47.8
SWD [24]	82.4	33.2	82.5	-	-	-	22.6	19.7	83.7	78.8	44.0	17.9	75.4	30.2	14.4	39.9	-	48.1
DADA [46]	89.2	44.8	81.4	6.8	0.3	26.2	8.6	11.1	81.8	84.0	54.7	19.3	79.7	40.7	14.0	38.8	42.6	49.8
SSF-DAN [12]	84.6	41.7	80.8	-	-	-	11.5	14.7	80.8	85.3	57.5	21.6	82.0	36.0	19.3	34.5	-	50.0
DISE [4]	91.7	53.5	77.1	2.5	0.2	27.1	6.2	7.6	78.4	81.2	55.8	19.2	82.3	30.3	17.1	34.3	41.5	48.8
AdaptPatch [44]	82.4	38.0	78.6	8.7	0.6	26.0	3.9	11.1	75.5	84.6	53.5	21.6	71.4	32.6	19.3	31.7	40.0	46.5
IntraDA [32]	84.3	37.7	79.5	5.3	0.4	24.9	9.2	8.4	80.0	84.1	57.2	23.0	78.0	38.1	20.3	36.5	41.7	48.9
Self-training (lower bound)	85.2	37.3	80.8	5.2	0.4	24.4	9.0	10.3	81.3	83.5	56.4	22.6	78.3	37.0	22.1	37.4	42.0	49.3
Ours - Random Selection	89.7	48.6	81.2	24.4	22.8	29.3	28.7	25.5	77.2	81.7	60.7	31.0	81.2	41.8	31.1	41.4	49.8	55.4
Ours - Active Selection	91.9	54.9	84.7	34.2	25.5	33.9	31.7	32.5	84.6	87.1	63.9	37.5	85.5	52.0	36.6	54.3	55.8	61.3
Ours - Full Labeling (upper bound)	93.5	66.3	85.5	39.0	37.0	36.3	37.0	53.7	85.6	89.1	65.4	40.8	85.2	56.4	39.4	60.9	60.7	**66.2**

traffic light, traffic sign, vegetation, terrain, sky, person, rider, car, truck, bus, train, motor bike, and bike.

- SYNTHIA: SYNTHIA-RAND-CITYSCAPES [37] as another synthetic dataset contains 9,400 fully annotated RGB images. Due to the large domain gap, number of samples of terrain, truck and train have limited distribution in the source domain. Thus 16 common classes in the experiments from SYNTHIA to Cityscapes dataset are considered in the experiment. In the process of testing, we take consideration of both 16 classes and 13 classes for better evaluation.

- Cityscapes: Cityscapes [8] provides images collected from real urban scenes with fine segmentation annotations. In the training set, there are 2,975 images with full segmentation maps. However, this work does not use any annotation maps for the training images. Finally we evaluate our model on the validation set, which contains 500 images with annotations.

Evaluation. In this work, we evaluate the semantic segmentation performance based on every category using the intersection-over-union metric, *i.e.*, IoU = TPO/(TPO + FPO + FNE) [13], where TPO, FPO, and FNE represent the number of true positive, false positive, and false negative pixels, respectively.

Implementation Details. Due to its effectiveness in minimizing the domain shift, we adopt the framework of [32] for unsupervised domain adaptation, in both two experiments of GTA5→Cityscapes and SYNTHIA→Cityscapes. For the first stage of unsupervised domain adaptation, the backbone of G_1 is a ResNet-101 architecture [18] with pretrained parameters from ImageNet [11]. With respect to the size of input data, we provide for the model G_1 the labeled source data of $1,280 \times 760$ and unlabeled target data of $1,024 \times 512$. The model G_1 is trained for totally 120,000 iterations. After training, G_1 is used to generate the corresponding prediction maps and entropy maps for all 2,975 images from Cityscapes training set. During the second stage of label acquisition, we divide each entropy map with a grid of 16×8 into 128 patches; the size of each patch is 64×64. On this basis, we randomly generated N points to be labeled. If the patch mean entropy is among top K highest, we send a request for human annotator to label these points. Otherwise, we directly transfer the pseudo labels from the prediction maps (from UDA) to the selected points. For the third stage of domain adaptation with point annotations, we train a semantic segmentation model G_2 which has same architecture as G_1, and a discriminator D_2 similar to D_1; the input target data are 2,975 Cityscapes training images with target point label $\hat{P}_t$. G_2 is trained with the pretrained parameters from ImageNet and D_2 is trained from scratch.

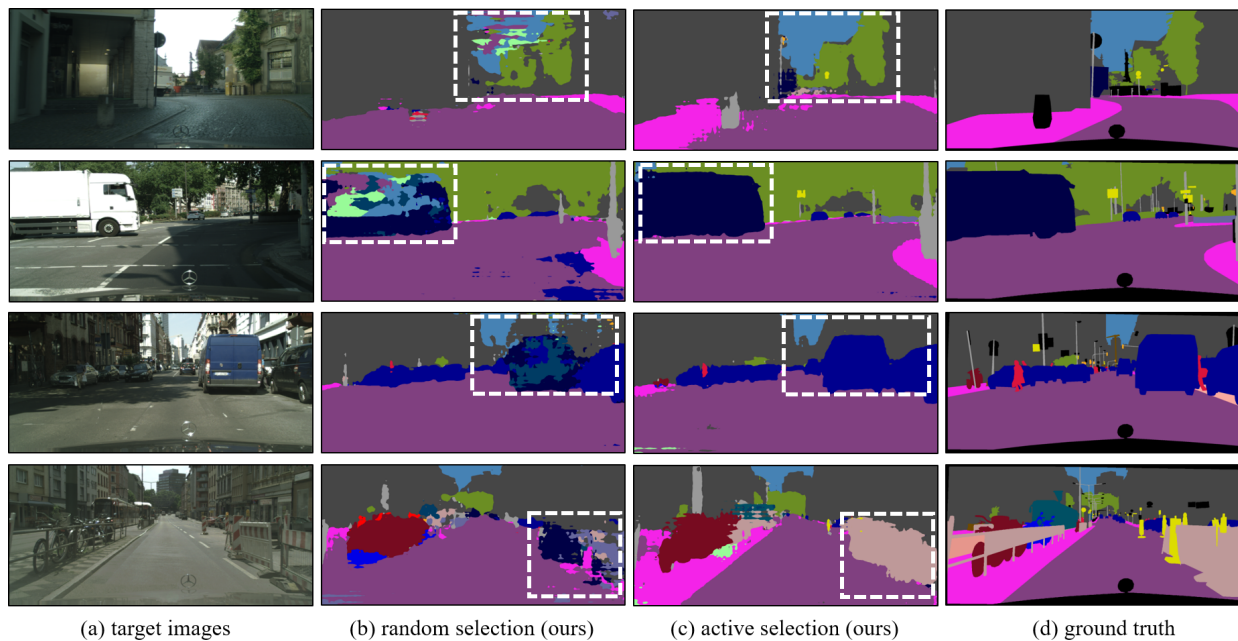Similarly to [32], [45] and [43], we utilize the multi-

(a) target images	(b) random selection (ours)	(c) active selection (ours)	(d) ground truth

Figure 3: The qualitative results of evaluation for GTA5 → Cityscapes. (a) and (d) are the images and corresponding ground truth annotations from Cityscapes validation set. (b) are the prediction maps from the model using random selection strategy. (c) are the prediction maps from the proposed model using active selection. Note that these experiments are conducted with number of selected patches is 10, and in each patch 5 random points are selected for oracle to annotate.

Table 3: The ablation study on hyperparameter K for patch selection. Note that the number of patches is 128. Thus the maximum value of K is 128. We select patches with top K highest mean entropy, and from each patch we randomly generate 5 points for oracle to annotate.

GTA5 → Cityscapes							
K	0	1	2	3	5	10	128
mIoU	47.7	49.2	49.3	49.5	50.1	51.5	60.1

level feature outputs from *conv4* and *conv5* for both the first and the second stage of domain adaptation. To train G_1 and G_2, we apply an SGD optimizer [3] with a learning rate of 2.5×10^{-4}, momentum 0.9, and a weight decay 10^{-4} for training G_1 and G_2. An Adam optimizer [22] with a learning rate of 10^{-4} is used for training D_1 and D_2.

4.2. Results

GTA5. We compare the semantic segmentation performance of our propose approach against state-of-the art UDA approaches on Cityscapes Validation set, as shown in Table 1 and Table 2. For a fair comparison, the baseline is adopted from DeepLab-v2 [6] with a ResNet-101 backbone.

To highlight the effectiveness of the proposed approach, we make a comparison of experiments from two different annotation strategy: random selection and active selection.

The random selection strategy is used to select 10 patches, within each patch 5 points are selected for human annotation. Different from it, active selection strategy is used to select the 10 patches with highest mean entropy value, within each patch 5 points are selected for human annotation. Overall, our model achieves 51.5% in mean IoU by using active selection. In the mean time, our model's performance only reach to 48.7% in mean IoU by using random selection. This experiment demonstrates that the proposed active selection strategy outperforms the random selection strategy in the label acquisition stage. To present the relevance of the proposed approach, we also conduct a comparison with self-training and full labeling method, as shown in Table 1. In the experiment of self-training method, we transfer the pseudo labels generated from UDA to the second stage of domain adaptation, without using any human annotations. In the experiment of full labeling method, we still generate 5 random points from each patch and we provide for all points human annotations, without using pseudo labels from UDA. By only using self-training method, the model only achieve 47.7% in mean IoU, while the baseline model IntraDA reach its performance to 46.5%. It shows that self-training method is a less effective method to minimize the domain shift in this problem setting. The full labeling achieves up to 60.1%, functioning as a upper bound.
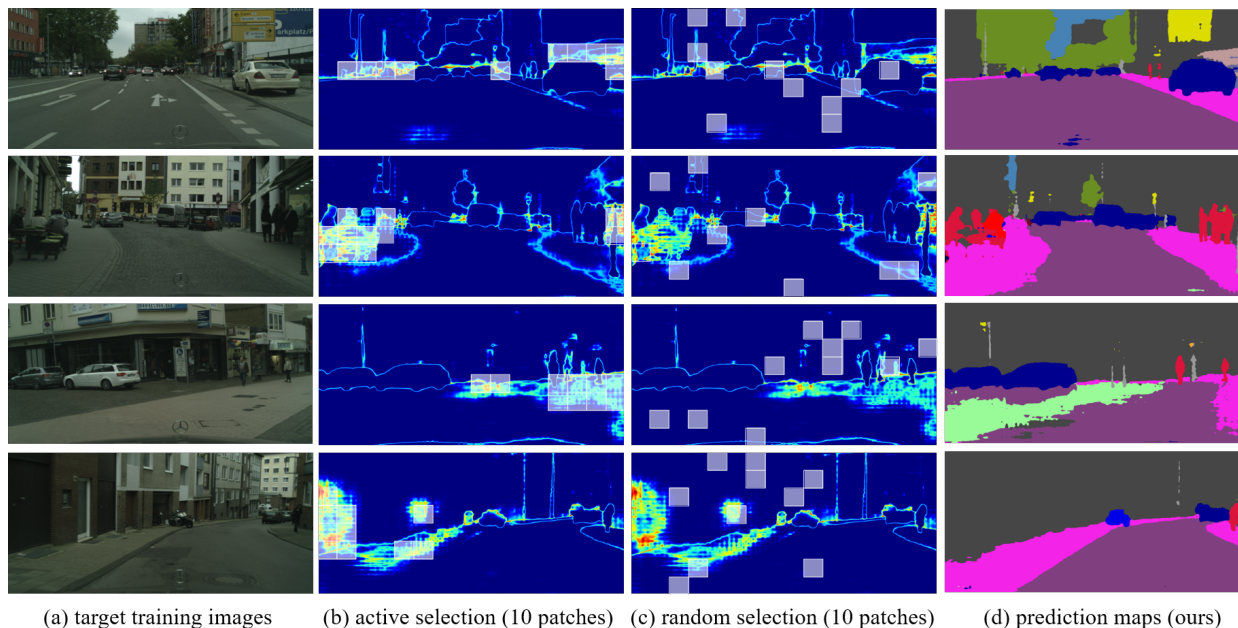
| (a) target training images | (b) active selection (10 patches) | (c) random selection (10 patches) | (d) prediction maps (ours) |

Figure 4: The examples of selection using active and random strategy in the evaluation for GTA5 → Cityscapes. (a) are the images from Cityscapes training set. (b) are the selected 10 patches from the entropy maps (from UDA) based on active strategy, shown as white rectangles. (c) are used to present the 10 selected patches from the entropy maps (from UDA) based on random strategy, also shown as white rectangles. (d) are the prediction maps generated from the proposed model using active selection. Note that in each selected patch, 5 random points are randomly generated for oracle annotation.

Analysis of Hyperparameter K We conduct an ablation study on the hyperparameter K in our experiment of GTA5 → Cityscapes. In Table 3, different values of K are used in the label acquisition system for patch selection. Remind that in the implementation process, the entropy map is divided by a grid of 16×8. Thus the maximum value of K is 128. For all experiments, we select patches with top K highest mean entropy, and from each patch we randomly generate 5 points for oracle to annotate. It is obvious to discover that with the value of K increase, the proposed model's performance also increase. This is because more supervision from human annotations are used during the training process.

SYNTHIA. So as to show the effectiveness of the proposed approach, we also conduct the experiments related to the adaptation from SYNTHIA → Cityscapes. In these experiments, we also adopt the same segmentation model based on DeepLab-v2 [6]. The proposed approach is evaluated on both 16-class and 13-class baselines. According to Table 2, the proposed approach with active selection strategy of 10 patches achieves 55.8% and 61.3% in mean IoU on 16-class and 13-class baselines, respectively. However, our approach with random selection strategy of 10 patches achieves 49.8% and 55.4% in mean IoU on both two baselines. These experimental results suggest that our approach

with active selection achieves higher performance than random selection strategy.

In addition, we also presents experimental results of self-training and full labeling method in Table 2. In the self-training experiment, the proposed model achieves 42.0% and 49.3% of mean IoU in both 16-class and 13-class baselines. However, IntraDA [32] reaches its performance up to 41.7% and 48.9% in both baselines. It shows that the self-training method generates marginal improvements of performance. The full labeling method achieves 60.7% and 66.2% in both baselines, functioning as a upper bound.

5. Conclusion

In this work, we propose a new domain adaptation framework for semantic segmentation with annotated points via active selection. First, we conduct an unsupervised domain adaptation of the model;from this adaptation, we use an entropy-based uncertainty measurement for target points selection. Finally, to minimize the domain gap, we propose a domain adaptation framework utilizing target points annotations. We present the experiments on synthetic data to real data in traffic scenarios. Experimental results on benchmark datasets shows the effectiveness of our approach against other domain adaptation approaches.

References

[1] Jiwoon Ahn and Suha Kwak. Learning pixel-level semantic affinity with image-level supervision for weakly supervised semantic segmentation. In *CVPR*, pages 4981–4990, 2018.

[2] Amy Bearman, Olga Russakovsky, Vittorio Ferrari, and Li Fei-Fei. What's the point: Semantic segmentation with point supervision. In *ECCV*, pages 549–565. Springer, 2016.

[3] Léon Bottou. Large-scale machine learning with stochastic gradient descent. In *Proceedings of COMPSTAT'2010*, pages 177–186. Springer, 2010.

[4] Wei-Lun Chang, Hui-Po Wang, Wen-Hsiao Peng, and Wei-Chen Chiu. All about structure: Adapting structural information across domains for boosting semantic segmentation. In *CVPR*, pages 1900–1909, 2019.

[5] Yu-Ting Chang, Qiaosong Wang, Wei-Chih Hung, Robinson Piramuthu, Yi-Hsuan Tsai, and Ming-Hsuan Yang. Weakly-supervised semantic segmentation via sub-category exploration. In *CVPR*, pages 8991–9000, 2020.

[6] Liang-Chieh Chen, George Papandreou, Iasonas Kokkinos, Kevin Murphy, and Alan L Yuille. Deeplab: Semantic image segmentation with deep convolutional nets, atrous convolution, and fully connected crfs. *TPAMI*, 40(4):834–848, 2017.

[7] Yuhua Chen, Wen Li, and Luc Van Gool. Road: Reality oriented adaptation for semantic segmentation of urban scenes. In *CVPR*, pages 7892–7901, 2018.

[8] Marius Cordts, Mohamed Omran, Sebastian Ramos, Timo Rehfeld, Markus Enzweiler, Rodrigo Benenson, Uwe Franke, Stefan Roth, and Bernt Schiele. The cityscapes dataset for semantic urban scene understanding. In *CVPR*, 2016.

[9] Ido Dagan and Sean P Engelson. Committee-based sampling for training probabilistic classifiers. In *Machine Learning Proceedings 1995*, pages 150–157. Elsevier, 1995.

[10] Jifeng Dai, Kaiming He, and Jian Sun. Boxsup: Exploiting bounding boxes to supervise convolutional networks for semantic segmentation. In *CVPR*, pages 1635–1643, 2015.

[11] Jia Deng, Wei Dong, Richard Socher, Li-Jia Li, Kai Li, and Li Fei-Fei. Imagenet: A large-scale hierarchical image database. In *CVPR*, pages 248–255. Ieee, 2009.

[12] Liang Du, Jingang Tan, Hongye Yang, Jianfeng Feng, Xiangyang Xue, Qibao Zheng, Xiaoqing Ye, and Xiaolin Zhang. Ssf-dan: Separated semantic feature based domain adaptation network for semantic segmentation. In *ICCV*, pages 982–991, 2019.

[13] Mark Everingham, SM Ali Eslami, Luc Van Gool, Christopher KI Williams, John Winn, and Andrew Zisserman. The pascal visual object classes challenge: A retrospective. *IJCV*, 111(1):98–136, 2015.

[14] Yarin Gal and Zoubin Ghahramani. Dropout as a bayesian approximation: Representing model uncertainty in deep learning. In *ICML*, pages 1050–1059, 2016.

[15] Yaroslav Ganin and Victor Lempitsky. Unsupervised domain adaptation by backpropagation. In *ICML*, pages 1180–1189. PMLR, 2015.

[16] Andreas Geiger, Philip Lenz, and Raquel Urtasun. Are we ready for autonomous driving? the kitti vision benchmark suite. In *CVPR*, pages 3354–3361. IEEE, 2012.

[17] Clément Godard, Oisin Mac Aodha, and Gabriel J Brostow. Unsupervised monocular depth estimation with left-right consistency. In *CVPR*, pages 270–279, 2017.

[18] Kaiming He, Xiangyu Zhang, Shaoqing Ren, and Jian Sun. Deep residual learning for image recognition. In *CVPR*, pages 770–778, 2016.

[19] Judy Hoffman, Eric Tzeng, Taesung Park, Jun-Yan Zhu, Phillip Isola, Kate Saenko, Alexei Efros, and Trevor Darrell. Cycada: Cycle-consistent adversarial domain adaptation. In *ICML*, pages 1989–1998. PMLR, 2018.

[20] Ajay J Joshi, Fatih Porikli, and Nikolaos Papanikolopoulos. Multi-class active learning for image classification. In *CVPR*, pages 2372–2379. IEEE, 2009.

[21] Tejaswi Kasarla, Gattigorla Nagendar, Guruprasad M Hegde, Vineeth Balasubramanian, and CV Jawahar. Region-based active learning for efficient labeling in semantic segmentation. In *WACV*, pages 1109–1117. IEEE, 2019.

[22] Diederik P Kingma and Jimmy Ba. Adam: A method for stochastic optimization. *arXiv preprint arXiv:1412.6980*, 2014.

[23] Alexander Kolesnikov and Christoph H Lampert. Seed, expand and constrain: Three principles for weakly-supervised image segmentation. In *ECCV*, pages 695–711. Springer, 2016.

[24] Chen-Yu Lee, Tanmay Batra, Mohammad Haris Baig, and Daniel Ulbricht. Sliced wasserstein discrepancy for unsupervised domain adaptation. In *CVPR*, pages 10285–10295, 2019.

[25] Di Lin, Jifeng Dai, Jiaya Jia, Kaiming He, and Jian Sun. Scribblesup: Scribble-supervised convolutional networks for semantic segmentation. In *CVPR*, pages 3159–3167, 2016.

[26] Jonathan Long, Evan Shelhamer, and Trevor Darrell. Fully convolutional networks for semantic segmentation. In *CVPR*, pages 3431–3440, 2015.

[27] Pauline Luc, Natalia Neverova, Camille Couprie, Jakob Verbeek, and Yann LeCun. Predicting deeper into the future of semantic segmentation. In *ICCV*, pages 648–657, 2017.

[28] Wenjie Luo, Alex Schwing, and Raquel Urtasun. Latent structured active learning. In *NeurIPS*, pages 728–736, 2013.

[29] Yawei Luo, Liang Zheng, Tao Guan, Junqing Yu, and Yi Yang. Taking a closer look at domain shift: Category-level adversaries for semantics consistent domain adaptation. In *CVPR*, pages 2507–2516, 2019.

[30] Radek Mackowiak, Philip Lenz, Omair Ghori, Ferran Diego, Oliver Lange, and Carsten Rother. Cereals-cost-effective region-based active learning for semantic segmentation. *arXiv preprint arXiv:1810.09726*, 2018.

[31] Andres Milioto, Philipp Lottes, and Cyrill Stachniss. Real-time semantic segmentation of crop and weed for precision agriculture robots leveraging background knowledge in cnns. In *ICRA*, pages 2229–2235. IEEE, 2018.

[32] Fei Pan, Inkyu Shin, Francois Rameau, Seokju Lee, and In So Kweon. Unsupervised intra-domain adaptation for semantic segmentation through self-supervision. In *CVPR*, pages 3764–3773, 2020.

[33] George Papandreou, Liang-Chieh Chen, Kevin P Murphy, and Alan L Yuille. Weakly-and semi-supervised learning of

a deep convolutional network for semantic image segmentation. In *ICCV*, pages 1742–1750, 2015.

[34] KwanYong Park, Sanghyun Woo, Inkyu Shin, and In So Kweon. Discover, hallucinate, and adapt: Open compound domain adaptation for semantic segmentation. *NeurIPS*, 33, 2020.

[35] Sujoy Paul, Yi-Hsuan Tsai, Samuel Schulter, Amit K. Roy-Chowdhury, and Manmohan Chandraker. Domain adaptive semantic segmentation using weak labels. In *ECCV*, 2020.

[36] Stephan R Richter, Vibhav Vineet, Stefan Roth, and Vladlen Koltun. Playing for data: Ground truth from computer games. In *ECCV*, pages 102–118. Springer, 2016.

[37] German Ros, Laura Sellart, Joanna Materzynska, David Vazquez, and Antonio M Lopez. The synthia dataset: A large collection of synthetic images for semantic segmentation of urban scenes. In *CVPR*, pages 3234–3243, 2016.

[38] Kuniaki Saito, Kohei Watanabe, Yoshitaka Ushiku, and Tatsuya Harada. Maximum classifier discrepancy for unsupervised domain adaptation. In *CVPR*, pages 3723–3732, 2018.

[39] Burr Settles and Mark Craven. An analysis of active learning strategies for sequence labeling tasks. In *EMLP*, pages 1070–1079, 2008.

[40] Inkyu Shin, Sanghyun Woo, Fei Pan, and In So Kweon. Two-phase pseudo label densification for self-training based domain adaptation. In *ECCV*, 2020.

[41] Yawar Siddiqui, Julien Valentin, and Matthias Nießner. Viewal: Active learning with viewpoint entropy for semantic segmentation. In *CVPR*, pages 9433–9443, 2020.

[42] Jong-Chyi Su, Yi-Hsuan Tsai, Kihyuk Sohn, Buyu Liu, Subhransu Maji, and Manmohan Chandraker. Active adversarial domain adaptation. In *WACV*, pages 739–748, 2020.

[43] Yi-Hsuan Tsai, Wei-Chih Hung, Samuel Schulter, Kihyuk Sohn, Ming-Hsuan Yang, and Manmohan Chandraker. Learning to adapt structured output space for semantic segmentation. In *CVPR*, pages 7472–7481, 2018.

[44] Yi-Hsuan Tsai, Kihyuk Sohn, Samuel Schulter, and Manmohan Chandraker. Domain adaptation for structured output via discriminative patch representations. In *ICCV*, pages 1456–1465, 2019.

[45] Tuan-Hung Vu, Himalaya Jain, Maxime Bucher, Matthieu Cord, and Patrick Pérez. Advent: Adversarial entropy minimization for domain adaptation in semantic segmentation. In *CVPR*, pages 2517–2526, 2019.

[46] Tuan-Hung Vu, Himalaya Jain, Maxime Bucher, Matthieu Cord, and Patrick Pérez. Dada: Depth-aware domain adaptation in semantic segmentation. In *ICCV*, pages 7364–7373, 2019.

[47] Qi Wang, Junyu Gao, and Xuelong Li. Weakly supervised adversarial domain adaptation for semantic segmentation in urban scenes. *TIP*, 28(9):4376–4386, 2019.

[48] Fisher Yu, Haofeng Chen, Xin Wang, Wenqi Xian, Yingying Chen, Fangchen Liu, Vashisht Madhavan, and Trevor Darrell. Bdd100k: A diverse driving dataset for heterogeneous multitask learning. In *CVPR*, pages 2636–2645, 2020.

[49] Yang Zhang, Philip David, and Boqing Gong. Curriculum domain adaptation for semantic segmentation of urban scenes. In *ICCV*, page 6, Oct 2017.

[50] Amy Zhao, Guha Balakrishnan, Fredo Durand, John V Guttag, and Adrian V Dalca. Data augmentation using learned transformations for one-shot medical image segmentation. In *CVPR*, pages 8543–8553, 2019.

[51] Hengshuang Zhao, Jianping Shi, Xiaojuan Qi, Xiaogang Wang, and Jiaya Jia. Pyramid scene parsing network. In *CVPR*, pages 2881–2890, 2017.

[52] Tinghui Zhou, Matthew Brown, Noah Snavely, and David G Lowe. Unsupervised learning of depth and ego-motion from video. In *CVPR*, pages 1851–1858, 2017.

[53] Yi Zhou, Xiaodong He, Lei Huang, Li Liu, Fan Zhu, Shanshan Cui, and Ling Shao. Collaborative learning of semi-supervised segmentation and classification for medical images. In *CVPR*, pages 2079–2088, 2019.